Mobility reduction and apparent activation energies produced by hopping transport in the presence of Coulombic defects

Mobility reduction and apparent activation energies produced by hopping transport in the presence of Coulombic defects

Franck Mady[1]**, Raphaël Renoud**[2] **and Philibert Iacconi**[1]

[1] LPES-CRESA (EA 1174), University of Nice-Sophia Antipolis, Parc Valrose, F-06108 Nice Cedex 2, France
[2] IREENA (EA 1770), University of Nantes, 2 rue de la Houssinière, BP92208, F-44322 Nantes Cedex 03, France

E-mail: franck.mady@unice.fr, raphael.renoud@univ-nantes.fr and iacconi@unice.fr

Abstract

A Monte Carlo simulation is proposed to study the mobility reduction due to Coulombic defects for hopping transport in a one-dimensional regular lattice. Hops between energetically equivalent sites and within an exponential distribution of energy levels are considered. In the absence of Coulombic wells, the calculations reproduce the well known features of Gaussian and highly dispersive transport respectively. When the field due to Coulombic potential wells is superimposed on the applied one, the macroscopic conduction features change dramatically. The computed apparent mobilities or transit times exhibit a Poole–Frenkel character and a modified Arrhenius temperature dependence. Their activation energy differs from the mean energy characterizing hops at the microscopic scale and it is found to depend on parameters such as the defect charge. This has important practical consequences for data interpretation.

1. Introduction

The electrical conduction in semiconductors and insulators is usually described in terms of multiple trapping (MT) and hopping. MT considers that conduction is due to the drift of electrons or holes in their respective bands of delocalized states, the motion being slowed down by a succession of capture on—and thermal release from—bandgap states (traps). By contrast, hopping transport describes tunnelling of a carrier from one localized state to another and does not require activation above a transport edge. Both mechanisms actually coexist and compete depending on the relative separations in energy and distance between traps. Even though this competition has been studied in detail by Blaise at thermodynamical equilibrium [1], a huge number of authors focused on transient behaviours related to pure MT or pure hopping. Both models succeed in producing the so-called anomalous dispersive transport observed in

disordered materials [2] and originally rationalized by the famous continuous time random walk (CTRW) theory of Scher and Montroll [3]. The latter predicts that transient currents following carrier excitation obey $I(t < t_T) \propto t^{-(1-\alpha)}$ and $I(t > t_T) \propto t^{-(1+\alpha)}$ depending on whether the time t is smaller or greater than the transit time t_T required to move a mean carrier across the sample, where α is the dispersion parameter lying between zero and unity.

Maybe the simplest hopping mechanism is the transport of small polarons, i.e. self-trapped charge carriers which move together with the surrounding structural deformation. The intrinsic motion of these quasi-particles can be described as a succession of jumps between energetically equivalent sites on a regular lattice, and the corresponding mobility can be cast into the following form, where F is the electric field [4]:

$$\mu(F) = \mu_0 \sinh\left(\frac{eF\lambda}{2k_BT}\right) \bigg/ \left(\frac{eF\lambda}{2k_BT}\right). \tag{1}$$

In equation (1), k_B is the Boltzmann constant, T is the absolute temperature and e is the magnitude of the electron charge. λ represents the mean distance between polaronic sites and μ_0 is the thermally activated zero-field mobility ($\mu_0 = \mu(0)$). Equation (1) is in fact valid at low fields and high temperatures. In the high field limit, the actual mobility is expected to vanish due to the decreasing probability of emission of the necessarily high number of phonons required to dissipate the energy $eF\lambda$ during a downward hop in energy (see Emin [5, 6]).

Hopping within an either positionally or energetically disordered system of localized states is an alternative model relevant for describing conduction in disordered materials. This much more complicated problem was extensively investigated both analytically and by simulation. Analytical efforts ranged from the stochastic theory of Scher and Lax [7, 8] to the recent mobility calculations of Arkhipov *et al* [9–11] in disordered organic semiconductors. Monte Carlo simulations were used, for instance, to study hopping between band-tail states of amorphous materials by considering a uniform distribution of traps with randomly distributed activation energies [12–15]. Silver *et al* [14] showed that a density of traps which decays exponentially with the trap depth ε according to $\exp(-\varepsilon/\varepsilon_c)$, where ε_c is a given mean level, could generate dispersive transport analogous to that of the CTRW theory. The dispersion parameter was found to be $\alpha = k_BT/\varepsilon_c$ at low fields [14, 16] and to become field dependent at high field. This can be explained by the proposal that high field effects are embodied in an effective temperature T_{eff} depending on both the lattice temperature and the field [12, 13, 15].

In the early 1970s, Gill [17] presented dispersive photocurrents measured on complexes of trinitrofluorenone and poly-*n*-vinylcarbazole (TNF:PVK). He found that the mobility evaluated from the inverse transit time was well fitted by an expression of the form

$$\mu(F, T) = \mu_0 \exp\left[-\frac{E_0 - \beta\sqrt{F}}{k_B}\left(\frac{1}{T} - \frac{1}{T_0}\right)\right]. \tag{2}$$

Since then, this unusual mobility has been observed in a wide class of materials, particularly in doped organic polymers, either for Gaussian or dispersive transport [17, 18]. The parameters E_0, T_0 and β can change with the material, but the $F^{1/2}$ dependence and the modified Arrhenius behaviour are universal. Experimental estimates of β were found to be the same for electrons and holes [17] and to be roughly equal to the Poole–Frenkel coefficient β_{PF}. The appearance of an effective temperature $(1/T - 1/T_0)^{-1}$ can be explained qualitatively by the 'modified Poole–Frenkel effect' of Jonscher and Ansari [19], who stipulated that hopping proceeds in the presence of a weak density of charged impurities, each of them extending over many localization centres. A detailed treatment of this situation and a theoretical support of equation (2) were more recently given by Rackovsky and Scher [18]. These authors considered a polaron executing a nearest-neighbour random walk on a two-dimensional lattice with a

central hole acting as a coulomb trap, by using the Holstein transition rates and Green's functions.

In this work, Gaussian motion of a small polaron and highly dispersive transport due to hopping in site-ordered exponential band-tails are successively considered (apparent mobility and transit time are retained as the relevant experimental observables respectively). The basic task is to show how the well known 'intrinsic' features of each model are modified by extrinsic charged defects responsible for Coulombic potential wells. It is demonstrated that the apparent mobility (2) is in fact consistent with the *simplest model* of one-dimensional hopping in the presence of Coulombic wells, and that it can fit both the extrinsic mobility and the extrinsic inverse transit time.

2. Simulation model

The simulation of hopping transport is generally based on the simplest possible model [9–16] formulated by Miller and Abrahams [20]. In the case of a one-dimensional treatment, jumps from site i to site k are then governed by the following hopping rate:

$$R_{ik} = \begin{cases} R_0 \exp\left(-\dfrac{2r_{ik}}{d}\right) \exp\left(-\dfrac{\Delta_{ik} - q(V_i - V_k)}{k_B T}\right) & \text{for } q(V_i - V_k) < \Delta_{ik}, \\ R_0 \exp\left(-\dfrac{2r_{ik}}{d}\right) & \text{for } q(V_i - V_k) > \Delta_{ik}. \end{cases} \tag{3}$$

In these expressions, r_{ik} and $\Delta_{ik} = \varepsilon_i - \varepsilon_k$ are respectively the spatial and the energy distances between the involved sites and d is the wavefunction localization length. V_i (respectively V_k) denotes the electrostatic potential experienced by a charge $q = \pm e$ located on site i (respectively k). R_0 is an attempt-to-escape frequency of the order of 10^{12} s^{-1} the magnitude of a typical phonon frequency. Note that the choice of R_0 only defines the timescale of the simulated experiment and does not affect the key results.

Simulations are carried out by considering a large number of sites placed along a regular one-dimensional lattice. The distance λ between sites is taken larger than d because carriers are no longer localized on separate sites if $\lambda < d$. The probability for a jump from site i to site j is given by

$$P_{ij} = \frac{R_{ij}}{\sum_{k \neq i} R_{ik}}, \tag{4}$$

and the mean time required for the hop is

$$\tau = \left(\sum_{k \neq i} R_{ik}\right)^{-1}. \tag{5}$$

The simulation thus requires two random numbers per hopping event. The first gives the destination of the hop in agreement with (4). The second specifies the time t for such a hop according to the density of probability $P(t) = \exp(-t/\tau)/\tau$.

The electric potential at a given position r is due to the superimposition of a uniform applied field F parallel to the hopping site array and of a uniform distribution of Coulombic wells produced by ionized defects (as donors or acceptors) located at r_i and charged with Q, each of them being of the form

$$V(r - r_i) = \frac{1}{4\pi \varepsilon_0 \varepsilon_r} \frac{Q}{\|r - r_i\|}, \tag{6}$$
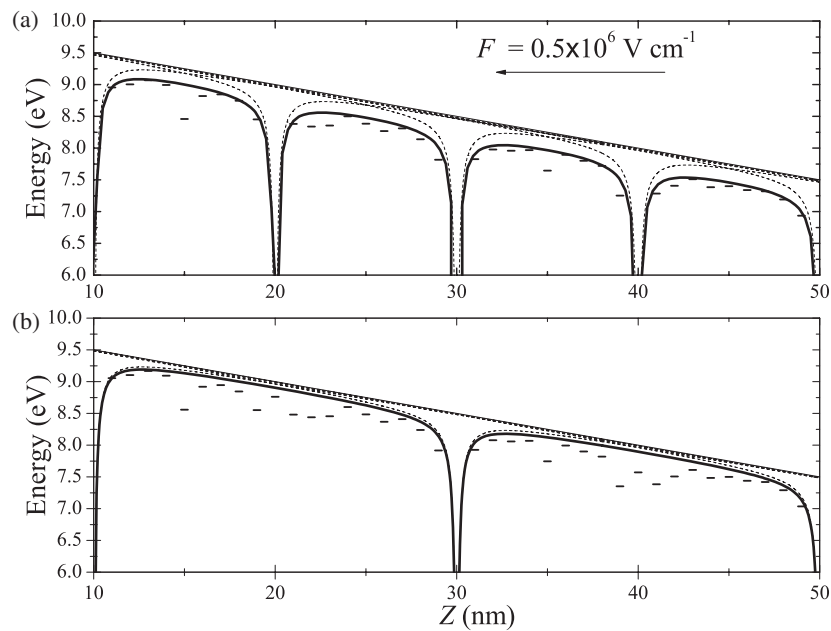
Figure 1. Mobility edge given by the electron potential energy against position for (a) $R_c = 10$ nm and (b) $R_c = 20$ nm, in the absence of Coulombic centres (straight line), by including the contribution of all ions (thick solid line) and by considering the nearest charged centre only (dashed lines). The dots represent a statistical distribution of localized states below the mobility edge.

where ε_0 and ε_r are the vaccum and the material relative permittivity respectively. Of course, most of these centres are actually neutralized because of the prohibitively high space charge that would accompany a high density of uncompensated ions. Thus, a reasonable consideration is that any particular carrier only feels the Coulombic field of the nearest ionized defect while the fields of more distant ones are effectively screened from it.

In practise, the history of each particle is followed from its injection on a site located at $Z = 0$ until it reaches a given sample thickness L. The retained results correspond to the average behaviour obtained from the simulation of several thousand independent 'trajectories'. According to this procedure, it is clear that filling or saturation of localized states is not taken into account. Particular attention is paid to the calculation of the mean velocity v of the carriers in the applied field direction. It provides information about their effective mobility after $\mu = v/F$.

Impurities are assumed to be separated by a constant distance R_c much greater than λ. The effect of the applied and Coulombic fields can be interpreted as a spatial deformation of the mobility edge above localized states, as illustrated for electrons in figure 1 for $\lambda = 1$ nm, $Q = +e$, $F = 0.5 \times 10^6$ V cm^{-1}, $\varepsilon_r = 4$, $R_c = 10$ and 20 nm. The thick line is the mobility edge in the absence of neutralization of distant centres, i.e. when *all* Coulombic centres contribute to the electron potential energy, whereas the dashed line corresponds to a localized electron, which only feels the potential of the nearest charged centre. The difference between these two situations is quite negligible for $R_c = 20$ nm and remains slight for $R_c = 10$ nm, that is for a high concentration of Coulombic centres (about 10^{18} cm^{-3}). Even if neutralization of distant ions is not explicitly included in calculations, hopping rates between localized states are therefore mainly perturbed by the first—and at worst the second—neighbouring defect, and not by more distant ions.

3. Small polaron hopping motion

In the small polaron problem, charge carriers get localized because they dig their own potential well by distorting the surrounding medium. The non-occupied sites can be regarded as zero energy centres ($\varepsilon = 0$), whereas the filled site can be characterized by the polaron activation energy $\varepsilon = \Delta$. Then, the intrinsic energy difference between the sites involved in a jump is constant, $\Delta_{ik} = \Delta$, and hops essentially take place between first neighbours.

Since the field-lowering of the small polaron activation energy is only one half of the difference in the site potential energies [4] the $q(V_i - V_k)$ term in (3) has to be replaced by $q(V_i - V_k)/2$. In the absence of Coulombic potential wells, the simulation of the polaron hopping motion leads to the same mobility as (1) at low fields, with

$$\mu(0) \propto \frac{e\lambda^2}{k_B T} \exp\left(-\frac{2\lambda}{d}\right) \exp\left(\frac{-\Delta}{k_B T}\right). \tag{7}$$

This result is normal since both the analytical theory and the simulation make use of one-dimensional models based on similar hopping rates [4, 5]. At high fields, the computed mobility departs from (1) and takes the decreasing form

$$\mu(F) = \frac{R_0 \lambda \exp(\frac{-2\lambda}{d})}{F}. \tag{8}$$

This law is satisfied when the field magnitude F exceeds the critical value $F_0 = 2\Delta/e\lambda$. Then, the condition $q(V_i - V_k)/2 > \Delta$ is always satisfied and the simulation mostly generates forward jumps at a rate $R = R_0 \exp(-2\lambda/d)$. Correspondingly, the effective velocity of hopping carriers becomes constant, equal to $R\lambda$, and the mobility obeys expression (8). This simplistic behaviour is inherent in the simulation model; the high field mobility derived by Emin [5] is most probably more physical.

Coulombic potential wells strongly affect the field and temperature dependence of the mobility as illustrated in figures 2 and 3. The data have been obtained from simulations carried out with $Q = +e$ (carriers are electrons), $\varepsilon_r = 4$, $R_c = 10$ nm, $R_0 = 10^{12}$ s^{-1}, $\lambda = 2$ nm, $d = 0.5$ nm, and $\Delta = 0.185$ eV. The plots of figure 2 still exhibit two regimes with respect to the applied field. The high field decrease has to be connected to the behaviour discussed above. Because of the potential wells, the electrons can feel electric fields which locally exceed F and experience energy variations greater than $eF\lambda$, even for the shortest jumps. Thus, the high field decrease now begins below $F_0 = 2\Delta/e\lambda$ ($F_0^{1/2} = 1.36$ MV$^{1/2}$ cm$^{-1/2}$ here). In the low field region, the plots are linear and the slopes depend on temperature. The straight lines intersect for a particular field, which is found to be about $F_0/2$ here. This indicates that the mobility no longer depends on temperature when the applied field is $\Delta/e\lambda$. As shown in figure 3, the temperature dependence of the mobility has similar properties: the plots are straight lines which intersect for a particular value T_0 (the mobility is therefore independent of the field when $T = T_0$).

The preceding features demonstrate that the simulation reproduces the phenomenological mobility (2) proposed by Gill [17] for $F \leqslant \Delta/e\lambda$ (low fields). The fit of the simulation results with this expression allows an estimate of the relevant parameters:

$$\mu_0 = 10^{-7} \text{ cm}^2 \text{ V}^{-1} \text{ s}^{-1}; \qquad E_0 = 0.295 \text{ eV};$$
$$\beta = 0.308 \text{ eV MV}^{-1/2} \text{ cm}^{1/2}; \qquad T_0 \approx 7500 \text{ K}.$$

The corresponding plots are drawn in dashed lines in figures 2 and 3. The β value is rather close to the Poole–Frenkel coefficient $\beta_{PF} = e(Q/\pi\varepsilon_0\varepsilon_r)^{1/2}$ for $Q = +e$ and $\varepsilon_r = 4$, i.e. $\beta_{PF} = 0.379$ eV MV$^{-1/2}$ cm$^{1/2}$ if $\varepsilon_0 = 8.85 \times 10^{-12}$ F m^{-1}. A better agreement was found from other calculations where each Coulombic well extends over ('contains') more localized
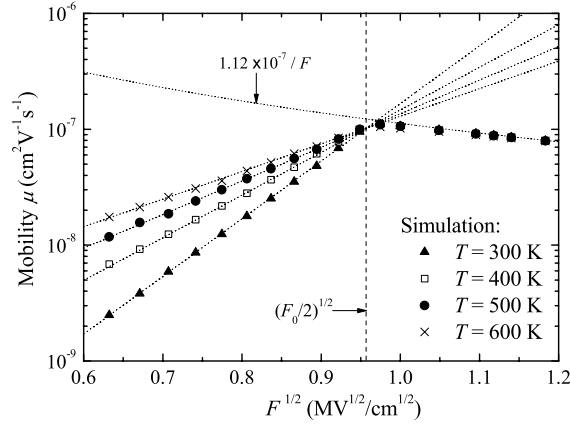
Figure 2. Mobility against the square root of the electric field at different temperatures and fits of the low field data with equation (1) (dashed lines).
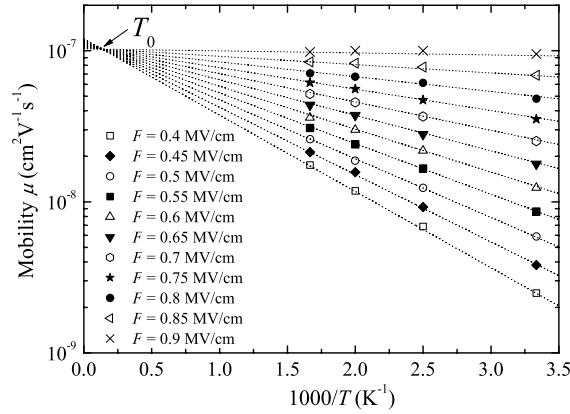
Figure 3. Mobility against the temperature at low field and fits with equation (1) (dashed lines).

states, that is with $R_c = 20$ nm ($\beta = 0.342$, $E_0 = 0.32$ eV) or $\lambda = 1$ nm ($\beta = 0.381$, $E_0 = 0.48$ eV). In addition, fits of simulation data carried out for $R_c = 10$ nm, $\lambda = 2$ nm but $Q = 2e$ lead to $\beta = 0.558$ (and $E_0 = 0.523$ eV), while the Poole–Frenkel coefficient is 0.536 in this case. General behaviours shown in figures 2 and 3 have been found to be remarkably reproducible for all sets of investigated parameters. The Poole–Frenkel behaviour, i.e. proportionality between the logarithm of the mobility and the square root of the field, is not the result of a presupposed mechanism. It is produced in a natural way due to the perturbations introduced by the Coulombic wells in the carrier hopping rates.

Since the mobility is temperature independent when $F \approx \Delta/e\lambda$, the macroscopic activation energy E_0 necessarily satisfies

$$E_0 \approx \beta\sqrt{\frac{\Delta}{e\lambda}}. \tag{9}$$

This expression is only deduced from numerical calculations and is not derived from physical or even mathematical arguments. It is roughly verified for all sets of reported parameters (Q, R_c, λ and Δ have been varied) within the error inherent in the simulation and fitting procedures. Perhaps a three-dimensional simulation would lead to a slightly different relation, but one can

nevertheless retain that the effective activation energy appearing at the scale of experiments is no longer the microscopic energy Δ as in equation (7). It now depends on Δ, but also on the mean distance λ between hopping sites and on the ion charge Q. This has a profound effect upon interpretation of experimental results since E_0 cannot be uniquely associated with a trap depth or a polaron binding energy.

4. Hopping in band-tails of disordered materials

We now consider hopping in site-ordered exponential band-tails [12–15]. The simulation differs from the small polaron study in the energy distribution of hopping sites. In order to reproduce the exponential density of localized states, proportional to $\exp(-\varepsilon/\varepsilon_c)$, an energy level ε_i is assigned to each localization site by drawing a random number γ_i uniformly distributed between zero and unity such that $\varepsilon_i = -\varepsilon_c \ln(1 - \gamma_i)$. In one dimension, this procedure has to be repeated before each particle injection to ensure the statistical reliability of the simulation. Hops are controlled by the competition between the spatial separation r_{ik} and the energy difference $\Delta_{ik} = \varepsilon_i - \varepsilon_k$ between sites. A carrier can now jump to a distant site whose energy is close to the occupied level instead of tunnelling to a neighbouring site.

As expected, the simulation shows that hopping transport in an exponential band-tail is highly dispersive. It is therefore convenient to present the results in terms of transient current $I(t)$ and transit time t_T. $I(t)$ is calculated from the knowledge of the instant number N_S of carriers contained in the sample and from the evaluation of their mean position $\bar{Z}$. To make the results independent of the number N_{tot} of simulated particles, $I(t)$ is expressed in the reduced form (10) with the dimension of an inverse time (s^{-1}):

$$I_{\text{simul}}(t) = \frac{1}{L} \frac{N_s}{N_{\text{tot}}} \frac{d\bar{Z}}{dt}. \tag{10}$$

The band-tail width has been fixed by setting $\varepsilon_c = 0.0862$ eV. Although arbitrary, this choice makes the low field dispersion parameter $\alpha = k_B T/\varepsilon_c$ easy to calculate (one then has $\alpha = T/1000$). The calculations also use the following parameters: $R_0 = 10^{12}$ s^{-1}, $\lambda = 1$ nm, $d = 0.5$ nm, $L = 200$ nm.

In the absence of Coulombic wells, the computed current reproduces the properties pointed out by prior research [12–15]. It is governed by an intricate interplay between temperature and field effects. For sufficiently low temperature and applied fields, the current satisfies the power law time dependence predicted by Scher and Montroll [3], where A and B are constants:

$$I(t) = \begin{cases} At^{-(1-\alpha)} & t < t_T \\ Bt^{-(1+\alpha)} & t > t_T. \end{cases} \tag{11}$$

The dispersion parameter is well given by $\alpha = k_B T/\varepsilon_c$ at low field but it becomes field dependent as the field is increased. This feature is illustrated in figure 4 by the simulated currents obtained for $T = 600$ K ($k_B T < \varepsilon_c$) and several applied fields ($F = 0.1$, 0.3 and 0.6×10^6 V cm^{-1}). For the lowest F value, the data are well fitted by (11) with $\alpha = 0.6$, as expected from $\alpha = T/1000$. For $F = 0.3$ and 0.6×10^6 V cm^{-1}, one has $\alpha = 0.62$ and 0.69 respectively. Transit times can be estimated from the fitted plots according to $t_T = (B/A)^{1/2\alpha}$. The values calculated for a significant set of temperatures indicate that the transit time is thermally activated: $t_T \propto \exp(E_a/k_B T)$. A reproducible activation energy E_a of about 0.2 eV was found for all the considered field.

Changes induced by the presence of the Coulombic potentials are illustrated in figure 5 for $Q = +e$, $R_c = 10$ nm, $T = 600$ K and $F = 0.2 \times 10^6$ V cm^{-1}. The Coulombic wells slow down the carrier motion and are responsible for a decrease in the instantaneous current

7
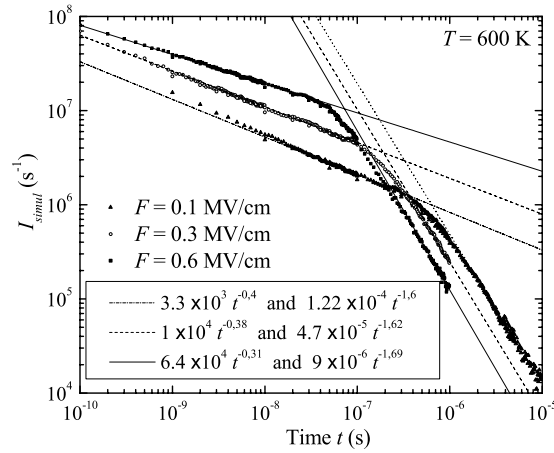
Figure 4. Simulated anomalous dispersive currents at $T = 600$ K. The fits by the power-law functions are shown. For each plot, the transit time is given by the intersection of the two straight lines.
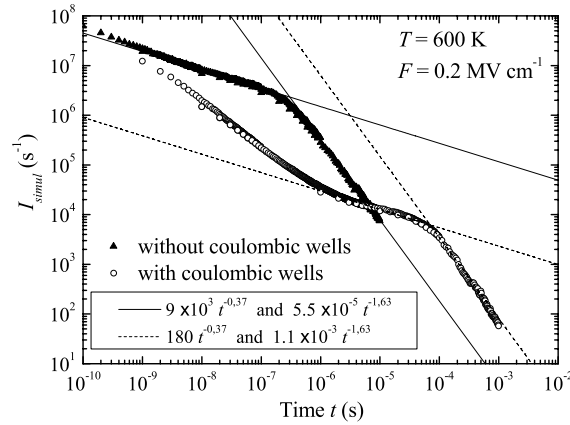

Figure 5. Simulated anomalous dispersive currents at $T = 600$ K and $F = 0.2 \times 10^6$ V cm^{-1} in the absence and in the presence of Coulombic defects. The fits show that the dispersion parameter is not modified.

as well as for an increase in the transit time. However, the current still obeys the power-law approximation (11) around the transit time for the same dispersion parameter $\alpha = 0.63$ as for intrinsic transport (the ionized defects do not affect dispersion). Calculations carried out at other T (500 K, 700 K) and F (0.3, 0.4 × 10^6 V cm^{-1}) confirmed that α is independent of the presence of charged defects.

Equation (11) does not provide a proper description of the current at short time because of the delay required to reach the steady-state regime of trap-limited transport. The regions where the current decay follows straight lines are therefore 'shortened' and this affects the accuracy of the estimate of coefficients involved in (11). Even if any small change in A or B (or also α) only leads to a small shift of the transit time location on the logarithmic scale, it yields a significant change in the corresponding value. The evaluation of the trap-modulated transit times t'_T has been carried out for a set of applied fields and temperatures. In each case,
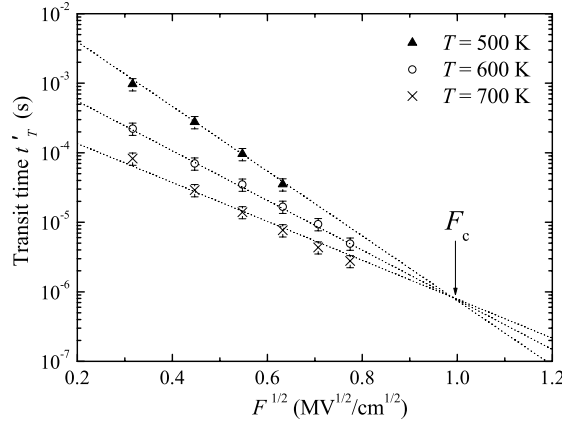
Figure 6. Transit-time against the square root of the electric field at different temperatures and fits of the low-field data with the inverse of equation (1) (dashed lines).
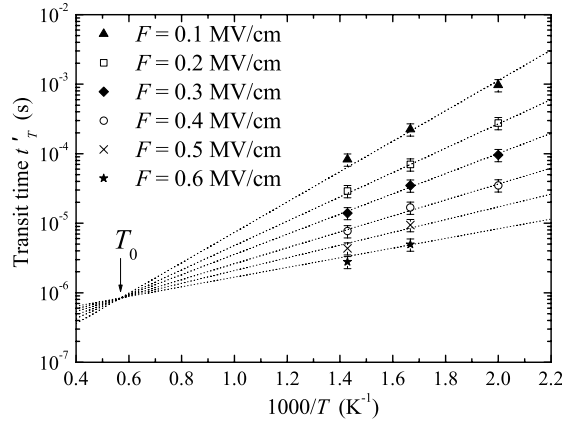
Figure 7. Transit-time against $1000/T$ at different fields and fits of the low-field data with the inverse of equation (1) (dashed lines).

the extreme straight lines (upper and lower limits) which could reasonably fit the data on both sides of the transit time were considered. We then deduced a corresponding transit time range and noticed that the discrepancies never exceed a 20% relative error. The plots of figures 6 and 7 show the values of t'_T taken at the middle of the error range, as a function of $F^{1/2}$ and $1000/T$ respectively, together with the error bars accounting for the overall 20% uncertainty. Note that two points are not reported for the lowest temperature and the highest fields considered here, that is at $T = 500$ K, $F = 0.5$ and 0.6 MV cm^{-1}. In these cases, field effects prevail over thermal ones and the steady-state trap-limited transport is not established before the first carrier transit. As a consequence, the related current plots depart markedly from straight lines and the transit times cannot be calculated in the framework of equation (11). Within the admitted error, impurity-limited transit times follow straight lines, which intersect for a particular field F_c and temperature T_0. They therefore satisfy

$$t'_T(F, T) = t'_{T_0} \exp\left[\frac{E_0 - \beta\sqrt{F}}{k_B}\left(\frac{1}{T} - \frac{1}{T_0}\right)\right]. \tag{12}$$

9

The fits shown in dashed lines have been obtained for the following parameters:

$$t'_{T0} = 8.4 \times 10^{-7} \text{ s}; \qquad E_0 = 0.64 \text{ eV};$$
$$\beta = 0.645 \text{ eV MV}^{-1/2} \text{ cm}^{1/2}; \qquad T_0 \approx 1760 \text{ K}.$$

There is now an appreciable difference between the β coefficient and the expected Poole–Frenkel one ($\beta_{PF} = 0.379$ eV MV$^{-1/2}$ cm$^{1/2}$). This discrepancy is not surprising with regard to the combined error introduced by the successive fits, but it prevents any definitive conclusion. The apparent activation energy E_0, related to the critical field F_c by $E_0 = \beta F_c^{1/2}$, differs from the mean energy ε_c of the band-tail states and is greater than the 0.2 eV energy obtained in the absence of Coulombic defects.

5. Discussion

It has been demonstrated in sections 3 and 4 that, statistically, the average mobility and transit time produced by the hopping rate (3) exhibit a Poole–Frenkel-like field dependence and a modified Arrhenius behaviour characterized by a critical temperature T_0. Two questions then remain: is the β coefficient of the phenomenological mobility (2) really the same as the Poole–Frenkel one and why? What is the physical origin of T_0 and what are the parameters which control its value?

The well known Poole–Frenkel (PF) model basically describes the classical emission of a carrier from an energy depth E_t at the centre of a Coulombic or neutral trap over a barrier lowered by a uniform external field [21, 22]. If an external field of magnitude F is turned towards the $-x$ direction, the potential energy of a carrier q at a distance x from a Coulombic centre can be written as

$$E_p(x) = \frac{\beta_{PF}^2}{4|x|q} + qFx. \tag{13}$$

The constant β_{PF} is defined as in section 3, that is here $\beta_{PF} = |q|(Q/\pi\varepsilon_0\varepsilon_r)^{1/2}$, so $\beta_{PF}^2/4|x|q^2$ is the Coulombic potential (6) in one dimension. The maximum of potential energy occurs at $x_0 = \beta_{PF}/2|q|F^{1/2}$, where $E_p = \text{sgn}(q)\beta_{PF}F^{1/2}$. Then, if the Coulombic contribution in (13) and the trap depth E_t are measured with respect to the potential energy at infinity, a trapped carrier will be emitted if it passes over a barrier $E_t - \beta_{PF}F^{1/2}$ and the thermal emission rate W from the Coulombic trap is

$$W = W_0 \times \exp\left(\frac{E_t - \beta_{PF}\sqrt{F}}{k_B T}\right). \tag{14}$$

Corrections to this simple theory generally result in multiplying the barrier lowering by a correction factor [22].

Let us now turn to the case of hopping transport. For the sake of simplicity, we focus here on the small polaron hopping motion for which the most probable hops take place between nearest neighbours (the hopping range is just λ, the mean distance between sites). If one assumes positive x_i, the potential energy variation accompanying a hop from site i to site k is given by equations (15) and (16) for forward and backward jumps respectively.

$$q(V_i - V_k) = qF\lambda\left[\frac{x_0^2}{x_i(x_i + \lambda)} - 1\right], \qquad x_k = x_i + \lambda, \tag{15}$$

$$q(V_i - V_k) = qF\lambda\left[1 - \frac{x_0^2}{x_i(x_i - \lambda)}\right], \qquad x_k = x_i - \lambda. \tag{16}$$

If the centres are positively charged and carriers are electrons ($Q > 0, q < 0$), a forward jump in space will correspond to an upward hop in energy if $q(V_i - V_k) < 0$ in (15), that is if x_i is smaller than the critical value x_c defined as

$$x_c = \frac{\lambda}{2}\left(\sqrt{1 + 4\left(\frac{x_0}{\lambda}\right)^2} - 1\right).$$ (17)

Similarly, (16) indicates that a backward jump in space will always correspond to a downward hop in energy if x_i is smaller than $x_c + \lambda$. As a consequence, carriers located on a site between 0 and x_c mainly undergo backward hops, i.e. towards the centre, and are likely to remain below x_c: they are 'trapped'. For carriers located on a site beyond $x_c + \lambda$, forward jumps correspond to downward hops whereas backward jumps are upward hops in energy. Thus, a carrier that has moved beyond $x_c + \lambda$ is likely to move away from the centre: it is emitted. For carriers between x_c and $x_c + \lambda$, both forward and backward jumps will produce downward hops in energy, but the backward jump will favour trapping while the forward jump will favour emission. The hop direction then depends on F, Q and λ. For instance, if λ or Q is such that $q(V_i - V_k)$ exceeds the polaron activation energy, equations (3)–(5) will make the probability of emission greater than that of capture.

A carrier bound to a Coulombic centre requires a certain average energy E_a to escape from the centre, just as in the classical PF effect, but this energy does not now refer to the edge of the barrier at x_0 (edge of the conduction band), but to some level between x_c and $x_c + \lambda$ at which the probability to escape is sufficiently high. One has

$$E_a = E_{a0} - \Delta E_a,$$ (18)

where E_{a0} is the average energy of electrons 'trapped' below x_c at equilibrium and ΔE_a is the barrier lowering, now given by the potential energy at x_c. Note that x_c and $x_c + \lambda$ both tend to x_0 when λ tends to zero, so the classical PF effect is then recovered (continuous distribution of states along the band edge). In normal conditions, when the Coulombic trap contains a significant number of localized sites between $x = 0$ and $x = x_c$ ($x_0/\lambda \ll 1$), one has

$$x_c = x_0 - \frac{\lambda}{2}\left(1 - \frac{\lambda}{4x_0}\right).$$ (19)

Therefore, x_c is slightly smaller than x_0. Correspondingly, the barrier lowering at x_c, given by equation (20), is slightly greater than for the classical PF.

$$\Delta E_a = \beta_{PF}\sqrt{F}\left(1 + \frac{1}{8}\left(\frac{\lambda}{x_0}\right)^2\right).$$ (20)

This result suggests that the barrier lowering is not exactly the same in the case of hopping transport as in the classical effect. The difference is not constant when the applied field varies (it decreases at low fields due to the increase of x_0), so the correction factor between β_{PF} and the constant coefficient β in (2) probably correspond to a mean correction averaged over the experimental field range. With regard to the experimental and fitting errors, one can reasonably retain that both coefficients are roughly the same. As regards our simulations, it is also difficult to discriminate between physical corrections and statistical and fitting errors in the deviations between β_{PF} and β. However, it has been mentioned in section 3 that increasing the number of centres within the Coulombic radius, i.e. decreasing λ/x_0 at all fields, well produces a β value much closer to the expected one β_{PF}: the β value was found to be 0.381 for $\lambda = 1$ nm instead of 0.308 with $\lambda = 2$ nm, while the theoretical β_{PF} value is 0.379.

The T_0 values reported in sections 2 and 4 are high, from about 1700 K for dispersive hopping transport up to 7500 K for small polaron motion. If experimental values of T_0 in the

range 550–660 K have been reported for electrons and holes by Gill in TNF:PVK [17], the theoretical model of Rackovsky and Scher [18] predicts values between about 500 K and almost infinity. Our T_0 values are of course included in this infinitely broad range, but comparison is difficult because of the differences in treatment: the T_0 values in [18] are shown to depend on the initial position of the carrier on the lattice with respect to the Coulombic centre, while this position is not retained as a parameter in our study. It is likely that simulations based on equation (3) would have yielded different T_0 values if the injection site ($Z = 0$ here, see section 1) had been varied. Actually, making an attempt at finding a straightforward interpretation of T_0, based on first principles and simple arguments, proves to be a very hard task. One may say that the modified Arrhenius behaviour is certainly associated with the field-assisted trapping of carriers since the derivative of the mobility (2) becomes a decreasing function of the field when $T > T_0$ [18]. This idea is consistent with the dependence of T_0 on the initial site because the latter also affects the trapping probability. To stand comparison with the experimentally measured T_0, which is of course independent of the initial position, the study would require a detailed calculation of the trapping and release probabilities averaged over a large number of initial sites. In this respect it seems that neither the present simulations nor the Rackovsky and Scher model are suitable for a proper examination of the modified Arrhenius law and of T_0.

6. Conclusion

The phenomenological mobility (2), first reported by Gill [17] for dispersive transport, was related to hopping in the presence of Coulombic traps a long time ago [19]. A formal derivation was given quite recently by Rackovsky and Scher, but with a substantial formalism and in the context of Gaussian transport only [18]. The present work demonstrates that this mobility is actually consistent with the simplest model of hopping motion in the presence of Coulombic potential wells at low field. It also extends the conclusion of [18] by showing that the basic characteristics of this mobility, namely the Poole–Frenkel field dependence and the modified Arrhenius behaviour, are not only obtained for the Gaussian motion of polarons, but also in the case of a highly dispersive intrinsic transport (hopping in band-tails of disordered materials), provided the mobility is estimated after $\mu \propto 1/t_T'$ as in the Gill experiments.

Trap-limited mobilities also exhibit a Poole–Frenkel field dependence in the multiple-trapping (MT) model of Gaussian transport (see [23, 24] for recent treatments of MT for Gaussian and dispersive transport). In this situation, however, the field-assisted lowering of the activation energy is initially assumed and included in the thermal release frequency W from Coulombic traps (equation (14)). It finally comes out in the apparent steady-state mobility because the latter is simply given by $\mu = \tau W$ for sufficiently deep traps, where τ is the mean lifetime before trapping. Then, the apparent activation energy of μ is necessarily the same as the microscopic trap energy E_t in W. As regards hopping, the Poole–Frenkel behaviour appears naturally, i.e. without underlying assumption, because hopping rates are perturbed by the Coulombic potential. In this respect, hopping transport is rather limited by the electrical perturbation due to defects than by trapping on a bandgap level in the MT sense. Then, the apparent activation energy E_0 in (2) is not simply related to a trap depth or to energies characterizing intrinsic transport. It depends on the extrinsic limiting defects through the coefficient β, comparable to the Poole–Frenkel coefficient, and is therefore proportional to the square root of the defect charge $Q^{1/2}$. It also depends on the critical field F_0 where the mobility (2) is temperature independent and so probably on the mean distance between localized states.

Properties of anomalous dispersive transport resulting from MT on an exponential trap distribution are also similar to that of hopping in an exponential band-tail. Both

mechanisms give rise to currents obeying equation (11) with the same dispersion parameter $\alpha = k_\mathrm{B}T/\varepsilon_\mathrm{c}$ [2, 23, 24]. Discrepancies between these models are expected at short time and high field. First, high field hopping transport is characterized by a field-dependent dispersion parameter which departs from the low field value. Second, multiple trapping can yield a specific current behaviour at short time [23, 24]. In all cases, discrimination between Coulombic trap-limited MT and hopping can be made because of the modified Arrhenius law characterizing hopping, provided the effective temperature $(1/T - 1/T_0)^{-1}$ clearly differs from T. The crossing temperatures T_0 reported in figures 3 and 7 are very high and confusion would be possible at low T in the situation of an experimental data analysis. A detailed study of the origin and of the dependence of T_0 and F_0 or F_c is beyond the scope of this paper, whose objective is mostly a qualitative demonstration of basic properties.

References

[1] Blaise G 2001 *J. Electrostat.* **50** 69–89
[2] Pfister G and Scher H 1978 *Adv. Phys.* **27** 747–98
[3] Scher H and Montroll E W 1975 *Phys. Rev.* B **12** 2455–77
[4] Austin I G and Mott N F 1969 *Adv. Phys.* **18** 41–102
[5] Emin D 1975 *Adv. Phys.* **24** 305–48
[6] Emin D 1991 *Phys. Rev.* B **43** 11720–4
[7] Scher H and Lax M 1973 *Phys. Rev.* B **7** 4491–502
[8] Scher H and Lax M 1973 *Phys. Rev.* B **7** 4502–19
[9] Arkhipov V I, Heremans P, Emelianova E V, Adriaenssens G J and Bässler H 2002 *J. Phys.: Condens. Matter* **14** 9899–911
[10] Arkhipov V I, Heremans P, Emelianova E V, Adriaenssens G J and Bässler H 2003 *Chem. Phys.* **288** 51–5
[11] Arkhipov V I, Heremans P, Emelianova E V, Adriaenssens G J and Bässler H 2004 *J. Non-Cryst. Solids* **338–340** 603–6
[12] Marianer S and Shklovskii B I 1992 *Phys. Rev.* B **46** 13100–3
[13] Cleve B, Hartenstein B, Baranovskii S D, Scheidler M, Thomas P and Baessler H 1995 *Phys. Rev.* B **51** 16705–13
[14] Silver M, Schoenherr G and Baessler H 1982 *Phys. Rev. Lett.* **48** 352–5
[15] Devlen R I, Antoniadis H, Schiff E A and Tauc J 1993 *Phil. Mag.* B **68** 341–55
[16] Grünewald M, Movaghar B, Pohlmann B and Würtz D 1985 *Phys. Rev.* B **32** 8191–6
[17] Gill W D 1972 *J. Appl. Phys.* **43** 5033–40
[18] Rackovsky S and Scher H 1999 *J. Chem. Phys.* **111** 3668–74
[19] Jonscher A K and Ansari A A 1971 *Phil. Mag.* **23** 205–23
[20] Miller A and Abrahams E 1960 *Phys. Rev.* **120** 745–55
[21] Arnett P C and Klein N 1975 *J. Appl. Phys.* **46** 1399–400
[22] Martin P A, Streetman B G and Hess K 1981 *J. Appl. Phys.* **52** 7409–15
[23] Mady F, Renoud R, Ganachaud J P and Bigarré J 2005 *Phys. Status Solidi* b **242** 2089–106
[24] Mady F, Reboul J M and Renoud R 2005 *J. Phys. D: Appl. Phys.* **38** 2271–5